Available online at www.sciencedirect.com

ScienceDirect

Energy Procedia 92 (2016) 845 – 851

Energy Procedia

6th International Conference on Silicon Photovoltaics, SiliconPV 2016

Identification of lifetime-limiting defects in as-received and heat treated seed-end Czochralski wafers

Elénore Letty[a,b]*, Jordi Veirman[a], Wilfried Favre[a], Mustapha Lemiti[b]

[a]CEA, LITEN, Department of Solar Technologies–National Institute of Solar Energy, F73375 Le Bourget du Lac, France
[b]Institut des Nanotechnologies de Lyon (INL), UMR 5270, University of Lyon, INSA-Lyon, 69621 Villeurbanne Cedex, France

Abstract

Major impurity-induced defects in Czochralski silicon are known to be related to oxygen and metallic elements. In this study we focus on seed-end wafers, and submit them to different solar cell process-related annealings. We find that in the as-received state, these seed-end wafers contain a central low carrier lifetime core. We demonstrate that the effective carrier lifetime in the as-received state is simultaneously governed by several defects including oxygen-related thermal donors and a defect deactivated at low temperature. After high temperature steps, a strong recombination center is formed in the central core. Preliminary results of effective carrier lifetime versus temperature measurements directly support oxygen precipitates to be limiting the carrier lifetime. In the light of all results, we propose a qualitative model for the high temperature behavior of these seed-end wafers.

© 2016 The Authors. Published by Elsevier Ltd. This is an open access article under the CC BY-NC-ND license
(http://creativecommons.org/licenses/by-nc-nd/4.0/).
Peer review by the scientific conference committee of SiliconPV 2016 under responsibility of PSE AG.

Keywords: Czochralski silicon; lifetime-limiting defects; oxygen; precipitation; thermal donors.

1. Introduction

It has been reported that 10 to 20% of Czochralski (Cz) wafers are affected by high concentrations of oxygen (O)-related defects and may not match photovoltaic (PV) specifications for high efficiency solar cells [1]. Regarding homojunction (HJ) cells, the efficiency drop was attributed to O precipitation during emitter diffusion [2]. Nevertheless, to our knowledge, the role of O precipitates (OP) in the efficiency drop was not directly observed, but

* Corresponding author. Tel.: +33-479-792-056.
E-mail address: elenore.letty@cea.fr

1876-6102 © 2016 The Authors. Published by Elsevier Ltd. This is an open access article under the CC BY-NC-ND license
(http://creativecommons.org/licenses/by-nc-nd/4.0/).
Peer review by the scientific conference committee of SiliconPV 2016 under responsibility of PSE AG.
doi:10.1016/j.egypro.2016.07.086

was rather inferred from the presence of high OP densities in areas where effective minority carrier lifetime (τ) is low. Complementary studies are thus needed. Recently, elegant techniques involving mid-temperature (T) annealings (~600°C) were developed to passivate defects in HJ process [3]. The applicability of these techniques to all Cz wafers requires however more data. Moreover, it is difficult to transfer these steps to other processes such as low T amorphous Si (a-Si) – crystalline Si heterojunction cells, since a-Si degrades at T>250°C. Therefore the study of defects in as-grown wafers remains fully relevant.

In this work, we investigate τ of seed-end Cz wafers, where formation of O-related defects such as OP and thermal donors (TD) is favored because of a high interstitial O concentration ($[O_i]$) associated to a slow cooling during crystal growth. We attempt to identify the τ -limiting defects in the as-received state as well as after different process-related annealings.

2. Experimental procedure

2.1. Sample preparation

Five sister wafers from the seed-end (solidified fraction = 4%) of an industrial phosphorus (P)-doped Cz ingot were studied. Using the OxyMap method described in [4] the following concentrations were measured at the center of a first wafer: $[P]=7\times10^{14}\,cm^{-3}$, $[O_i]=1.15\times10^{18}\,cm^{-3}$. The as-grown TD concentration ([TD]) varied from $1.2\times10^{15}\,cm^{-3}$ at the center to $8\times10^{13}\,cm^{-3}$ at the periphery. The 4 remaining wafers were submitted to the process steps described in Fig. 1.

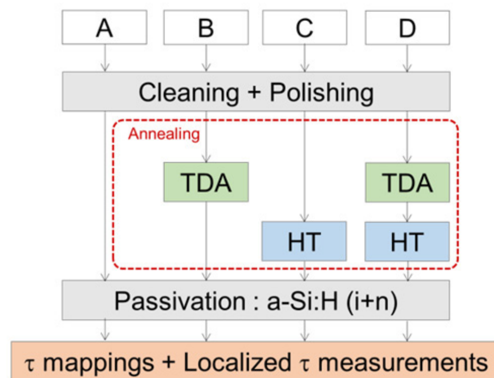

Fig. 1. Process flow. TDA stands for "Thermal Donors Annihilation" and HT for "High Temperature" annealing.

Polishing was performed using an alkaline solution. Identical annealings, either TD Annihilation (TDA) or high T annealing (HT), were performed simultaneously. TDA is a 10 min annealing at 750°C, allowing TD suppression [5]. The HT annealing (900°C, 1h30) mimics the thermal profile of both boron and P diffusions. Passivation stacks of a-Si layers (intrinsic and n-type) on both wafer surfaces were deposited by PECVD (T~200°C). This stack allows high passivation quality to be achieved ($S_{eff} < 2\ cm.s^{-1}$).

2.2. Sample characterization

τ mappings were obtained using Microwave Photoconductance Decay (μPCD). At the wafer center, measurements of injection- and T- dependent τ (IDLS and TDLS) were carried out using a SINTON-WCT120 equipment. TDLS was performed between 25°C and 160°C. Following the procedure detailed in [6], TDLS allows to get information on energy levels introduced by the dominant recombination-active centers in a wafer. The technique is based on a simplification of the τ expression related to SRH recombination channels (τ_{SRH}) at low injection level (Δp) as a function of T. τ_{SRH} is obtained from τ according to Eq. 1.

$$\frac{1}{\tau} = \frac{1}{\tau_{SRH}} + \frac{1}{\tau_{\text{int}}} + \frac{1}{\tau_{surf}} \quad (1)$$

Where τ_{int} is the lifetime limited by intrinsic recombination channels (Auger and radiative recombinations) and τ_{surf} is the lifetime limited by surface recombinations.

From [6], in the case of an energy level introduced close to the conduction or valence bands, the τ_{SRH} limited by this recombination-active center can be expressed as Eq. 2. This expression is however valid only in low Δp conditions, at sufficiently high T, considering a shallow center (close to one of the bands) and if the density of recombinant centers is inferior to a threshold density N_{crit} whose value is a function of carriers densities, energy level position and ratio of capture cross sections [7].

$$\tau_{SRH}^{LLI}(T) \approx \frac{T}{\sigma_p(T)} \exp\left(-\frac{\Delta E_t}{k_B T}\right) \quad (2)$$

Here $\sigma_p(T)$ represents the T-dependence of the capture cross section for holes, and ΔE_t is the position of the energy level relative to the priori unknown closest band, i.e. $\Delta E_t = E_t - E_V$ or $\Delta E_t = E_C - E_t$ [6]. As we do not know a priori the recombination-active center in our samples, we assumed that capture cross-section for holes is T-independent. Under this assumption, the slope of the Arrhenius plot obtained by TDLS indicates the value of ΔE_t introduced by the recombination-active center. TDLS alone does not however give information on the half of the band gap where the energy level is located.

The influence of intrinsic recombination channels on the carrier lifetime was calculated using Richter’s model and subtracted from our measurements of τ as a function of T [8]. Regarding the quality of passivation compared to the measured τ, τ_{surf} was neglected. Estimated τ_{surf} (>3 ms) is indeed largely higher than measured τ, and we can thus consider that τ is essentially limited by τ_{SRH} and τ_{int} (Eq. 1). The τ_{SRH} was then extracted at low Δp, as required by the procedure detailed above: $\Delta p = n_0/10 = 7\times10^{13}$ cm^{-3}, where n_0 is the electron concentration (n_0=[P]+2[DT]). Prior to TDLS measurements, the wafers were annealed at 200°C during 7h in ambient atmosphere, to avoid any transient effect in the passivation quality.

3. Results

3.1. Identification of defects in as-received samples

μPCD mappings show the presence of a low τ core (LLC) in as-received wafers (Fig. 2 (a)). Similar observations were recently reported for early bodies of Cz ingots [9]. After TDA, τ is homogenized and reaches values higher than 1.5 ms all along the wafer (Fig. 2 (b)). The LLC in wafer A corresponds to the area where [TD] is the highest.

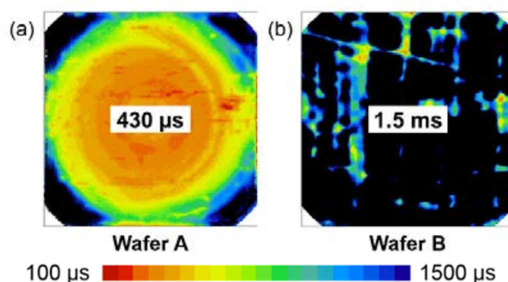

Fig. 2. μPCD τ mappings performed on passivated wafers (a) as-received; (b) after TDA. τ in the central zone measured with a SINTON-WCT120 at $\Delta p = 1.10^{15}$ cm^{-3} is indicated in white boxes.

Using an in-house model to simulate recombination at TD [10], we computed the τ in the LLC of wafer A considering TD as the τ-limiting defect (Fig. 3), using Richter's model for τ_{int} calculation [8]. τ_{surf} and its variation with Δp were estimated from measurements on high-quality passivated Float-Zone samples. The associated error on computed τ is related to the high lateral gradient of [TD] in the LLC. Below $\Delta p=1.10^{15} cm^{-3}$, the recombinant centers density is higher than the critical concentration N_{crit} [7] leading to inapplicability of the model.

We observed a significant discrepancy between prediction and measurement, suggesting the presence of another defect. To identify this second defect, we performed specifically on wafer A isochronal annealings of 30 min between 100°C and 300°C (50°C step). Low [O_i] wafers (both Float-Zone and Cz) were used as references in order to monitor surface passivation variations. The slight observed variations at highest T were used to correct the τ data by a passivation degradation factor. We found that τ almost doubled in the LLC of wafer A after the 250°C annealing (Fig. 3). This low deactivation T points toward a vacancy-related defect [11]. The remaining gap between predictions and experiment could be due to a third defect. We did not however investigate this possibility any further, as the gap may as well be related to experimental and modelling uncertainties.

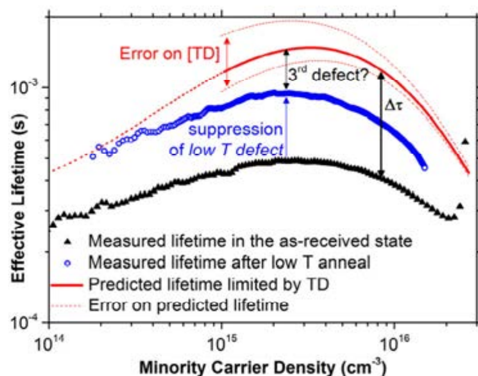

Fig. 3. Measured and predicted τ in the LLC of wafer A.

3.2. Identification of defects in HT annealed samples (wafers C and D)

A HT step induced a strong material degradation in the region where the LLC was observed on as-received wafers (Fig. 4 (a)). Performed after TDA, this HT step leads to an even stronger τ drop (Fig 4 (b)). Contrary to the results of Section 3.1, TD cannot be responsible for the LLC observed here since they were destroyed during the TDA and/or HT step. Therefore, we demonstrate that care must be taken when attributing a given defect to an observed LLC, as the responsible defect can be manifold.

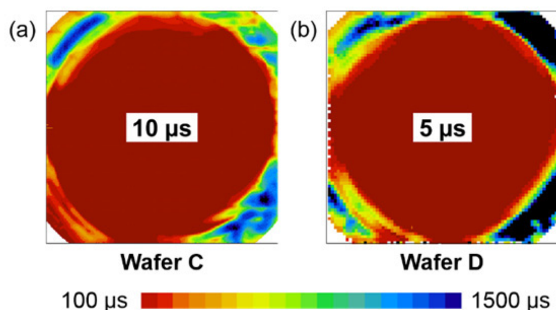

Fig. 4. μPCD τ mappings performed on passivated wafers (a) after HT (b) after TDA+HT. τ in the central zone measured with a SINTON-WCT120 at $\Delta p=1.10^{15}$ cm^{-3} is indicated in white boxes.

In order to investigate the underlying defect after HT steps, TDLS measurements were carried out (Fig. 5). As already mentioned in paragraph 2.2, τ_{surf} was neglected and, as a first blind guess, capture cross sections were considered T-independent (Eq. 2). We concluded from Fig. 5 that the τ-limiting defect in the LLC is the same in both wafers (same slopes). This defect introduces a recombination active level around ΔE_t=0.20 eV, which is compatible with OP level measured by Deep Transient Level Spectroscopy (ΔE_t=0.2-0.3 eV) [12]. Our results thus suggest that OP may be the τ-limiting defect in these studied heat treated seed-end wafers. Nevertheless, it has been more recently reported that lifetime-killing OP, which were stronger recombinant centers when strained [13], introduce two independent recombinant centers, labeled defect 1 and defect 2, at the following energy levels: $E_{t1}=E_v+0.22$ eV and $E_{t2}=E_c-0.08$ eV [14,15].

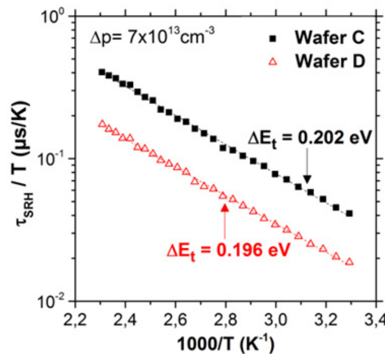

Fig. 5. Arrhenius plot of TDLS measurements in the LLC of wafers C and D. Energy levels position calculated from the slopes (Eq. 2) are indicated.

The consideration of both energy levels makes the usual TDLS approach difficult to apply. To circumvent this issue, we chose to compute the theoretical Arrhenius plot that one should get if these two levels were present in our samples and to compare the computed slope with measured ones, rather than extracting energy levels from the experimental plot. The τ_{SRH} limited by recombinations related to the OP, $\tau_{SRH,OP}$, is defined by Eq. 3 where $\tau_{SRH,1}$ is the carrier lifetime limited by SRH recombinations related to defect 1, and $\tau_{SRH,2}$ the one related to defect 2.

$$\frac{1}{\tau_{SRH,OP}} = \frac{1}{\tau_{SRH,1}} + \frac{1}{\tau_{SRH,2}} \tag{3}$$

Rearranging the standard SRH statistics [7], the lifetime limited by SRH recombination in n-type Si can be written as:

$$\tau_{SRH}(T) = \tau_{p0}(T)\left(1 + \frac{n_1(T)}{n_0(T)} + \frac{1}{k}\frac{p_1(T)}{n_0(T)}\right) \tag{4}$$

Where n_1 and p_1 are the equilibrium concentrations of electrons and holes, respectively, when the Fermi level coincides with the energy of the recombination center, and τ_{p0} is defined as:

$$\tau_{p0}(T) = \frac{1}{\alpha_p(T)N_t} \tag{5}$$

α_p is the capture coefficient for holes, and k is the ratio of the capture coefficients ($k=\alpha_n/\alpha_p$ with α_n the capture coefficient for electrons). N_t is the density of recombination-active defects. We expressed directly the quantity $N_t\,\alpha_p$ as a function of $N_{strained}$ (density of strained OP) and $\Delta[O_i]$ ($[O_i]$ consumed during precipitation), as developed in [15]. We did not measure $N_{strained}$ and $\Delta[O_i]$, but fortunately their absolute value has no effect on the slope of the simulated Arrhenius plot. Thus, for the computation, we picked arbitrary values. Finally, we checked for both levels that the defect densities N_{crit} above which SRH simplified model cannot be applied anymore [7] were significantly greater than the estimated densities in our samples. SRH recombination parameters of the two defects introduced by OP have been described in [14,15] and are summarized in Table 1.

Table 1. SRH parameters from [14,15].

Parameter	Value – Defect 1	Value – Defect 2
E_t	$E_V + 0.22$ eV	E_C - 0.08 eV
k	157	1/1200
$N_t\,\alpha_p$ (300 K)	(3×10^{-11} cm^3/s) $N_{strained}^{1/3}$ $\Delta[O_i]^{2/3}$	(3×10^{-8} cm^3/s) $N_{strained}^{1/3}$ $\Delta[O_i]^{2/3}$
Activation energy of α_p	0.20 eV	-
Activation energy of α_n	-	0.14 eV

TDLS measurements were performed at T<200°C. We thus considered n_0 to be independent of T. We assumed the position of each level, the ratio of the capture coefficients k and the densities of each defect to be T-independent.

The resulting theoretical Arrhenius plot is presented in Fig. 6. A slope of 0.23 eV is obtained, in very close agreement with the experimental slopes. Among other uncertainty sources, the relative error of 15% can be related to the expression of $N_t\,\alpha_p$ as a function of $N_{strained}$ and $\Delta[O_i]$. Indeed, the parameterization that was used here was derived from measurements on samples where precipitation was forced and preceded by a tabula rasa annealing. In that way, the OP population in our sample can somehow differ from that used for SRH parametrization in [15], in terms of sizes and shapes of OP. Our results nevertheless bring direct evidence that OP are responsible for the τ drop in the LLC of wafers C and D after HT step. It is the first time to our knowledge that the direct implication of OP in the τ drop on process-related annealed wafer is reported.

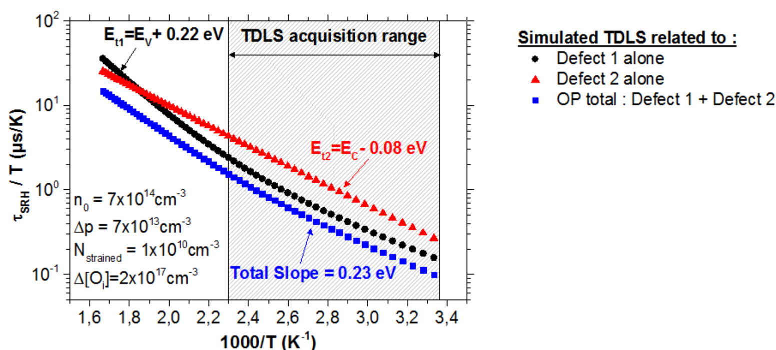

Fig. 6. Simulated Arrhenius plots representing T-behavior of τ related to defect 1 alone (black circles), defect 2 alone (red triangles) and to OP (blue squares). Parameters used for the simulation are indicated in the white box. Energy level position calculated from the slope is indicated.

3.3. Qualitative precipitation model

We tentatively propose a qualitative model that explains our findings, in the light of all previous results. The TDA performed at 750°C would allow some small nuclei present in as-received wafers to grow (alongside some larger nuclei). In that way they could reach a sufficient size to survive a HT step whereas these smallest nuclei would be killed during the rising ramp of HT annealing on wafer C. Density of strained OP would thus be higher in wafer D leading to a smaller τ. The high τ in wafer B indicates that after TDA the nuclei have not reached a

sufficient size to be strained and therefore do not limit τ. In addition, TD and the *low T defect* identified in wafer A are annihilated leading to an overall high τ.

4. Conclusions and outlook

It was shown that as-received seed-end wafers contain a LLC resulting from several defects including TD and *low T defect*. After TDA, a high and homogeneous τ is obtained. The strong τ drop after HT steps (with and without TDA) were qualitatively explained by the growth of large strained OP, the TDA enhancing the precipitation through drifting of the nuclei population to higher sizes, able to survive HT. To our knowledge, we evidenced for the first time the direct implication of OP in the τ drop on wafers submitted to process-related annealing. We underlined that the attribution of a given defect to an observed LLC is not straightforward and requires care, as many different defects can lead to a similar τ pattern (here: TD, OP, maybe the *low T defect*). Future work is planned in order to get further information about nuclei size and density in as-received wafers. We also intend to study the *low T defect*.

References

[1] Bronsveld PCP, Manshanden P, Gutjahr A, Koppes M, Coletti G and Romijn IG. The effect of n-Pasha processing on bulk wafer quality. 31st edition of the European Photovoltaic Energy Conference and Exhibition 2015.
[2] Haunschild J, Broisch J, Reis IE and Rein S. Cz-Si wafers in solar cell production: Efficiency-limiting defects and material quality control. Photovoltaics International 2012;15: 40-46.
[3] Hallam B, Chan C, Abbott M and Wenham S. Hydrogenation of defect-rich n-type Czochalski silicon and oxygen precipitates. Solar Energy Materials & Solar Cells 2015;141:125-131.
[4] Veirman J, Dubois S, Enjalbert N and Lemiti M. A Fast and Easily Implemented Method for Interstitial Oxygen Concentration Mapping Through the Activation of Thermal Donors in Silicon. Energy Procedia 2011;8:41–46.
[5] Stein HJ, Hahn SK and Shatas SC. Rapid thermal annealing and regrowth of thermal donors in silicon. Journal of Applied Physics 1986:59: 3495.
[6] Rein S. Lifetime spectroscopy: a method of defect characterization in silicon for photovoltaic applications. Springer Series in Materials Science (Springer-Verlag, Berlin Heidelberg). Vol. 85; 2005.
[7] Macdonald D and Cuevas A. Validity of simplified Shockley-Read-Hall statistics for modeling carrier lifetimes in crystalline silicon. Physical Review B 2003:67:075203.
[8] Richter A, Glunz SW, Werner F, Schmidt J and Cuevas A. Improved quantitative description of Auger recombination in crystalline silicon. Physical Review B 2012:86:165202.
[9] Gaspar G, Juel M, Søndenå R, Pascoa S, Di Sabatino M, Arnberg L and Øvrelid EJ. On the shape of n-type Czochralski silicon top ingots. Journal of Crystal Growth 2015;418:176-184.
[10] Tomassini M, Veirman J, Varache R, Letty E, Dubois S, Hu Y, Nielsen Ø. Recombination activity associated with thermal donor generation in monocrystalline silicon and effect on the conversion efficiency of heterojunction solar cells. Journal of Applied Physics 2016:119:084508.
[11] Watkins GD. Intrinsic defects in silicon. Materials Science in Semiconductor Processing 2000;3:227–235.
[12] Mallik K, Falster RJ and Wilshaw PR. Schottky diode back contacts for high frequency capacitance studies on semiconductors. Solid-State Electronics 2004;48:231-238.
[13] Murphy JD, Bothe K, Olmo M, Voronkov VV and Falster RJ. The effect of oxide precipitates on minority carrier lifetime in p-type silicon. Journal of Applied Physics 2011:110:053713.
[14] Murphy JD, Bothe K, Krain R, Voronkov VV and Falster RJ. Parameterisation of injection-dependent lifetime measurements in semiconductors in terms of Shockley-Read-Hall statistics: An application to oxide precipitates in silicon. Journal of Applied Physics 2012;111(11):113709.
[15] Murphy JD, Al-Amin M, Bothe K, Olmo M, Voronkov VV and Falster RJ. The effect of oxide precipitates on minority carrier lifetime in n-type silicon. Journal of Applied Physics 2015;118(21):215706.